ECS Transactions, 111 (6) 1239-1247 (2023)
10.1149/11106.1239ecst ©The Electrochemical Society

Investigation of the Reaction Mechanisms in $La_{1-x}Sr_xCo_{1-y}Fe_yO_3$ Electrode by DFT Calculations

C. Hartmann[a], G. Geneste[b,c], K. Saravanabavan[a,d], and J. Laurencin[a]

[a] Univ. Grenoble Alpes - CEA/LITEN, 17 rue des Martyrs, 38054, Grenoble, France
[b] CEA, DAM, DIF, F-91297 Arpajon, France
[c] Université Paris-Saclay, CEA, Laboratoire Matière en Conditions Extrêmes, 91680 Bruyères-le-Châtel, France
[d] Genvia SAS, Plaine Saint Pierre 34500 Béziers, France

$La_{1-x}Sr_xCo_{y-1}Fe_yO_{3-\delta}$ (LSCF) is a widely used oxygen electrode in Solid Oxide Cells (SOCs). Despite its high electrochemical activity combined with a good mixed ionic and electronic conductivity, it is prone to a phase decomposition upon operation decreasing the global cell performance. However, the underlying mechanisms for the reaction mechanism and the degradation are still not precisely understood and require investigations at atomic scale. Therefore, Density Functional Theory (DFT) calculations are used to better unravel the mechanisms occurring in the electrode. In particular, the interaction of the dioxygen gas with the AO-terminated (100) surface is studied. In this context, the oxygen reduction reaction is decomposed in a series of elementary steps including oxygen vacancy formation, adsorption of the dioxygen molecule on the bare surface and into a surface vacancy accompanied with the formation of intermediate oxygen species, followed by the dissociation and incorporation into the bulk. The calculations have been carried out at two different Cobalt contents (y=0.125 and y=0.25).

Introduction

Solid Oxide Cells (SOCs) are electrochemical devices working at high temperatures for a clean hydrogen and electricity production in electrolysis (SOEC) and fuel cell modes (SOFC), respectively. The SOC consists of two porous electrodes separated by a dense electrolyte, which is a pure ionic conductor. The so-called 'hydrogen electrode' and 'oxygen electrode' are supplied with the H_2 and O_2, respectively. At each electrode, the following half reactions can occur respectively, i.e. ($H_2 + O^{2-} \leftrightarrow H_2O + 2e^-$) and ($½O_2 + 2e^- \leftrightarrow O^{2-}$), whereby the released electrons are exchanged via the external circuit. SOCs have attracted a growing attention thanks to its high efficiency without the use of expensive catalysts. Although SOCs could play a key role in the energy transition, its commercialization at large scale is still limited due to performance and degradation issues.

The state of the art oxygen electrode $La_{1-x}Sr_xCo_{1-y}Fe_yO_3$ (LSCF) exhibits a high electrochemical activity combined with a good mixed ionic and electronic conductivity. Nevertheless, LSCF is prone to decompose upon operation with a Strontium segregation at the surface reducing the cell performance over time [1]. To date, the driving force of Sr segregation in LSCF and its impact on the cell performance is still not precisely understood. It has been suggested that it could be related to the evolution of oxygen

vacancies under anodic and cathodic polarization [2]. However, in order to unravel these intricate phenomena, it is still necessary to investigate the mechanisms that take place in the electrode at the atomic scale. In the present paper, we study the underlying mechanisms of the oxygen reduction reaction ($½O_2 + 2e^- \rightarrow O^{2-}$) using density functional theory (DFT) calculations. First-principles studies have suggested that the (001) surface must be the most stable low index orientation [3]. Furthermore, low energy ion scattering experiments have indicated that the surface should be AO terminated [4] (where the A-site of the LSCF perovskite correspond to La or Sr). Therefore, the current study is carried out on the AO-terminated (001) surface.

The present article is structured as follows. First, the LSCF slab in absence of adsorbed species (bare surface) has been studied. Second, the formation of oxygen vacancies in the LSCF have been investigated at surface, sub-surface and sub-sub-surface. Third, the oxygen reduction reaction has been divided into a succession of elementary steps: (i) the adsorption of the O_2 gas on the bare surface versus the adsorption into a surface oxygen vacancy and (ii) the dissociation and incorporation due to a second oxygen vacancy in the sub-surface.

Computational Details

Spin-polarized Kohn-Sham DFT calculations were performed as implemented in ABINIT software [5]. In this code, the resolution of the Kohn-Sham equations is carried out using periodic boundary conditions. Therefore, the elementary mechanisms have been investigated using a slab model of the LSCF system. The slabs has been built with a symmetry axis at the center layer to avoid a macroscopic electric field due to the charged surfaces. It is constituted by 9 layers of type (AO BO2 AO BO2 AO BO2 AO BO2 AO), corresponding to a stack of 2x2x4 pseudo-cubic unit cells. Besides, to model the surface, a vacuum layer of around 23 Å is added between the symmetric slab and its periodic image (Figure 1. a). For one case, the thickness of the vacuum layer has been increased to 61 Å in order to test convergence with respect to energy and force. Note that the drawback of such a symmetric slab is that it becomes non-stoichiometric. The surface mechanisms have been investigated for two different Cobalt concentrations, i.e. y=0.125 and 0.25 and 7 Sr in the supercell. In the case of y=0.125 additionally supercells with 8 Sr were simulated. The Projector-Augmented Wave (PAW) formalism was used and the corresponding data set taken from the Jollet-Torrent-Holtzwarth (JTH) table [6]. Hybrid PBE0 functional was applied within the PAW sphere to better account for exchange-correlation for transition metal *d* electrons. Outside the PAW spheres the GGA functional was used [7],[8]. The k-point sampling was done with a 4x4x1 mesh grid. A plane-wave cut-off of 20 Hartrees (Ha) was used. The Broyden-Fletcher-Goldfarb-Shanno (BFGS) minimization was employed for structural optimization and convergence stopped when all the atomic forces lied below $2x10^{-4}$ Ha/bohr.

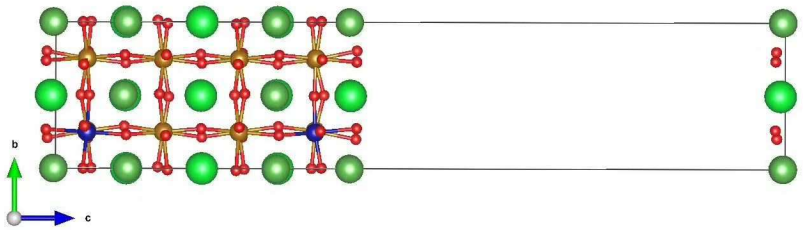

Figure 1. LSCF slab with atomic positions as obtained after structural optimization for a Cobalt content of y=0.125 (dark green=La, bright green=Sr, red=O, orange=Fe, blue=Co).

Results

The performance of the LSCF electrode depends on the flux of oxygen ions that crosses the electrolyte/electrode interface. This flux depends on the ability of the oxygen electrode to provide or receive oxygen ions to or from the electrode. If the oxygen electrode is a mixed ionic electronic conductor, such as $La_{1-x}Sr_xCo_{1-y}Fe_yO_3$ (LSCF), the oxygen flux can be provided/received via the surface path at the triple phase boundary and the bulk path [9]. The oxygen flux at the electrolyte/electrode interface is thus dependent on the surface and bulk properties of the oxygen electrode material. In other words, it depends on the catalytic properties of the electrode material for the oxygen incorporation/ex-corporation as well as the transport properties at the surface and in the bulk. First, the slab with a bare surface has been investigated before studying the elementary mechanisms occurring during the oxygen reduction reaction.

Bare surface

The structural optimization has been initialized with the ideal pseudo-cubic positions. After relaxation, an octahedral tilting is observed (Figure 1.). The tilting slightly breaks the symmetry of the slab. In order to quantify the effect of a possible resulting electrostatic dipole field, the vacuum space has been increased from 23 to 61 Å for one configuration (y=0.125, 8Sr) and the convergence in energy and forces have been compared. The difference in energy is of the order of 1 meV and the maximal difference in the absolute force is of the order of $3x10^{-4}$ Ha/bohr. This value lies slightly above the used convergence criterion in the structural optimization, i.e. $2x10^{-4}$ Ha/bohr. However, as the difference is small, it has been assumed that the tilting symmetry breaking might be considered as negligible.

The substitution of La^{3+} by Sr^{2+} is an acceptor doping leading to the formation of electron holes in the system. These electron holes appear as localized states within the bandgap for all studied Co and Sr concentrations, (Figure 2.). This is in agreement with the experimental finding that LSCF has a thermally activated electronic conductivity associated to a polaron hopping process [10]. The minimum bandgap is found to be reduced when the Cobalt content is increased from 0.125 to 0.25 (cf. Table 1.).

TABLE I. Fundamental band gap for spin up and spin down channels in eV for LSCF for different Cobalt and Strontium contents.

	Band gap (eV)		Simulated structure
LSCF (y=0.125, 7Sr)	0.58 (up)	0.36 (down)	Pseudo-cubic slab
LSCF (y=0.125, 8Sr)	0.44 (up)	0.51 (down)	Pseudo-cubic slab
LSCF (y=0.250, 7Sr)	0.18(up)	0.53 (down)	Pseudo-cubic slab

Please note that the number of electron holes does not equal to the number of strontium ions within the non-stoichiometric slab. This behavior is due the additional AO surface layer in the symmetric slab that results in supplementary electrons compensating some of the holes. Therefore, in the case of 7 Sr, effectively only three holes exist, whereby one of these holes is localized on a cobalt ion and the other holes are localized on iron ions. This distribution of electron holes over Co and Fe ions might not be unique and other possible distribution with similar energy might exists. However, this possibility has not been investigated in the present work.

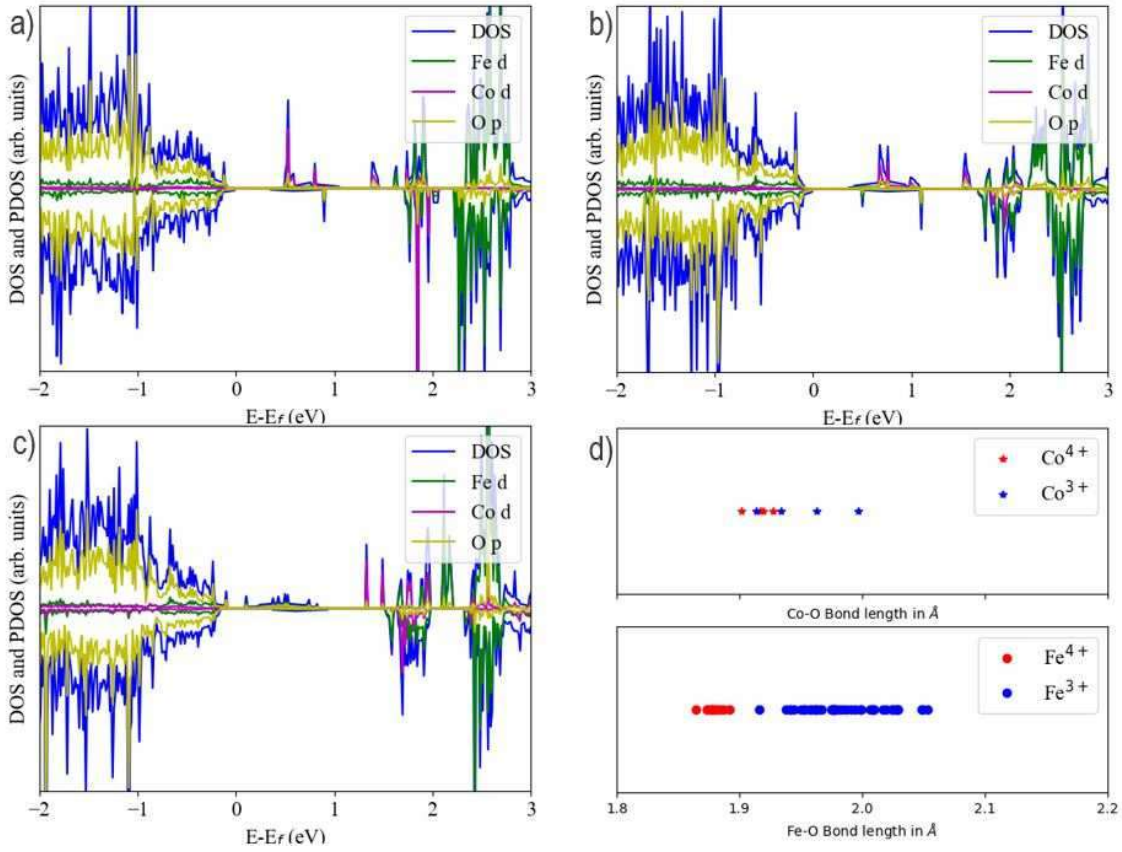

Figure 2. The Density Of State (DOS) and Projected Density Of State (PDOS) as a function of energy with respect to the Fermi energy E_f, for the bare surface with a Cobalt content of 0.125 for a) with 7 Sr in the supercell and b) with 8 Sr in the supercell, and c) with a Cobalt content of 0.25 and 7 Sr. d) the four NN TM-O bond lengths.

In Figure 3. the isosurfaces of the probability density of wavefunctions associated to the electron hole localized on an iron and a cobalt ion are shown. They show the hybridization of the Fe *3d* and Cobalt *3d* orbitals with the O *2p* orbitals. Compared to cobalt, the iron ions are much strongly hybridized with oxygen ions and the shape of the

probability density is very similar to the one found in the parent material LSF as detailed in [11]: the poalron is extended over five atoms (i.e. one iron and four nearest neighbor (NN) oxygen). While the probability density associated to the Fe hole state is oriented along the O-Fe bonds, in the case of Co, the probability density is found to occupy the space in between the O-Co bonds and is less strongly hybridized with O *2p* orbitals (Figure 3. b)). By analyzing the 3*d* occupation matrices of the iron and cobalt on which an electron hole is localized, their occupancies are found to be reduced and therefore the oxidation state are interpreted as +4. The localization of a hole state is accompanied with a distortion of the lattice, especially in the case of iron the bonds towards the four neared neighbor (NN) oxygen are noticeable shorted (cf. Figure 2. d)).

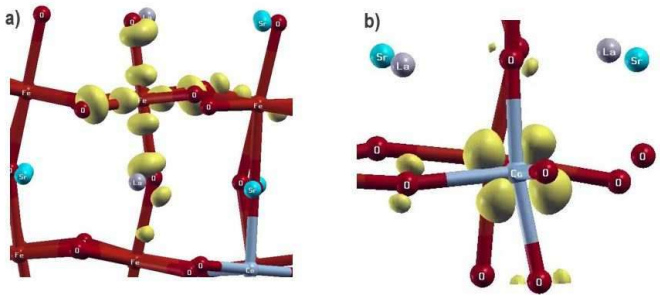

Figure 3. Isosurfaces (20% of the maximum value) of the probability density of the wave functions associated to a hole state localized on a) iron and b) cobalt in the slab with y=0.125 and 8 Sr.

Oxygen vacancy formation

Oxygen vacancies play a crucial role in the reaction mechanism, as they are involved in the oxygen incorporation (or excorporation) process in LSCF and they are necessary for the ionic conductivity. Two oxygen vacancies have to be considered in the simulation in order to conserve the symmetry of the slab (and they have to be equally distributed with respect to the symmetry axis of the slab). The vacancy formation energies E_v for surface, sub-surface and sub-sub-surface are listed in Table II and are calculated according to:

$$E_v \approx ½ (E_{slab,Vö} - E_{slab} + E_{O_2}), \quad [1]$$

where E_{slab}, $E_{slab,Vö}$ *and* E_{O_2} denote the energy of the slab without oxygen vacancy, the energy of the slab with two symmetrically distributed oxygen vacancies and the energy of the dioxygen gas molecule.

TABLE II Oxygen vacancy formation energies in eV and nearest neighbor (NN) transition metal cation for a Cobalt content of 0.25 and 0.125.

	NN TM cation	Ev (7Sr,y=0.25)	Ev (7Sr,y=0.125)	Ev (8Sr,y=0.125)
Surface 1	Fe	1.76	1.49	1.07
Surface 2	Co	2.21	1.80	1.41
Sub-surface 1	Fe-Fe	1.58	1.35	-
Sub-surface 2	Fe-Co	2.17	1.40	1.32
Sub-Sub-surface 1	Fe-Fe	1.72	1.86	-
Sub-Sub-surface 2	Co-Fe	1.39	1.26	-

The oxygen vacancy formation energies are all positive, and thus oxygen vacancy formation present an endothermic process at 0K. Within our slab model, no clear relationship in the oxygen vacancy formation energy with respect to the surface and different sub-surfaces has been found. Either the differences in formation energies are more strongly influenced by its local environment or this observation might be biased by the different approximations and constraints made in the calculations.

A noticeable decrease in the oxygen formation energy is obtained when the strontium content is increased from 7 Sr to 8 Sr. This can partially be explained by the following mechanism. In the case of 7 Sr, only 3 holes exist in the bare slab, while in the case of 8 Sr, 4 holes are present. During oxygen vacancy formation, two electrons per vacancy are delivered to the system (thus in total four electrons). For the system with 7 Sr, three electrons are counterbalanced by the three holes, while the remaining electron has to be placed in the conduction band. In all simulated cases for 7 Sr, the creation of a cobalt ion of lower oxidation state is observed (Co^{2+}) suggesting that the conduction band of Co is lower in energy with respect to Fe. In the case of 8 Sr, however, the number of delivered electrons equals the number of holes in such a way that it is not necessary to lower the Co oxidation state (from Co^{3+} to Co^{2+}).

Adsorption of the O_2 molecule

First, the adsorption on the bare surface without surface vacancies has been investigated. Thereby only vertically adsorbed O_2 molecules at bridge and top surface sites have been considered. Adsorption energies E_A are calculated by the following expression:

$$E_A \approx ½ (E_{slab,ads}-E_{slab}-2E_{O_2}) \quad [2]$$

where $E_{slab,ads}$ denotes the energy of the slab with two molecules adsorbed on the top and the bottom surfaces and which are symmetrically distributed with respect to the symmetry axis of the slab. The adsorption energies range between -0.6 and 0.02 eV and are in most cases negative suggesting that molecular adsorption is possible for most cases on the bare surface (Table III). The bond lengths of the adsorbed dioxygen molecules are longer than that of the isolated dioxygen molecule and adopt values between 1.25-1.31 Å. Note that the configurations marked with an asterisk in Table III correspond to the case where one of the vertically adsorbed molecule spontaneously flip toward a horizontally position. As these values are more negative, it suggests that horizontally adsorbed molecules might be more favorable. However, we cannot give the exact adsorption energy as the configuration contains in these cases both a horizontally and vertically adsorbed O_2 molecule.

TABLE III Adsorption energy E_A in (eV), bond length in (Å) and nearest neighbor (NN) A-site cation for molecular adsorption on the bare surface at different adsorption sites (bridge and top).

	NN A-site	E_A (eV)		Bond length (Å)	
		y=0.125	y=0.25	y=0.125	y=0.25
Bridge 1	La-Sr	-0.12	0.02	1.27	1.27
Bridge 2	La-La	-0.60*	-	1.27/1.31	-
Top 1	Sr	-0.24	-0.23	1.25	1.25
Top 2	La	-0.51*	-0.18	1.29/1.26	1.26

Furthermore, the adsorption directly into a surface oxygen vacancy has been calculated as follows:

$$E_A \approx ½ (E_{slab,Vö,ads}-E_{slab}-2E_{O_2}), \quad [3]$$

where $E_{slab,Vö,ads}$ denotes the energy of the slab with two symmetrically adsorbed dioxygen species into the surface vacancies. The computation for the adsorption directly into a surface vacancy has been performed considering either a superoxide (O_2^-) or a peroxide (O_2^{2-}) state. After structural optimization, only the peroxide states were found to be stable while the superoxides converged spontaneously towards peroxides. Besides, it appears from this analysis that the peroxide does not stand out of the (100) plane, but leans towards the direction between two A-site surface ions as shown in Figure 4.. The oxygen-oxygen bond length of the peroxides adopt a characteristic value of about 1.5 Å. In addition, the formation of a peroxide O_2^{2-} is accompanied with a charge transfer from the slab towards the adsorbed species increasing the number of hole states in the slab.
From this study, it could be suggested that the superoxide might not exist at the LSCF AO terminated (001) surface. Nevertheless, one cannot exclude that the superoxide state might exist as an exited state (if the Born-Oppenheimer surface of the peroxide remains lower than the minimum of the Born-Oppenheimer surface associated to the superoxide). Furthermore, Gao *et al.* have succeeded to stabilize the superoxide state onto the LSCF surface [4]. Therefore, further calculations should be performed to investigate if the superoxide species can co-exist with peroxide on the electrode surface.

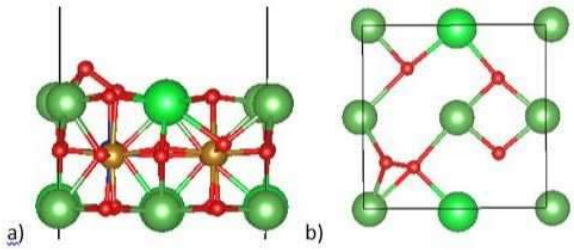

Figure 4. a) Side and b) top view of the peroxide adsorbed into a surface oxygen vacancy.

The adsorption energies for the oxygen molecule into surface vacancy are listed in Table IV. The adsorption energies are much lower than in the case of the adsorption on the bare surface and take values between -2.28 and -1.29 eV. Therefore, the surface oxygen vacancies present very reactive sites for oxygen adsorption. In other words, it can be claimed that the presence of surface oxygen vacancies on the LSCF surface strongly promote the oxygen adsorption.

TABLE IV Adsorption energy E_A in (eV), bond length and nearest neighbor (NN) TM- cation for molecular adsorption into an oxygen vacancy.

	NN TM-site	E_A (eV)			Bond length		
		y=0.125 (7Sr)	y=0.125 (8Sr)	y=0.25 (7Sr)	y=0.125 (7Sr)	y=0.125 (8Sr)	y=0.25 (7Sr)
Peroxid 1	Fe	-1.29	-1.48	-2.07	1.49	1.47	1.48
Peroxid 2	Co	-2.28	-2.06	-2.08	1.49	1.49	1.49

Dissociation and incorporation

In the previous section, the formation of a peroxide by directed adsorption into a surface vacancy has been considered. Eventually, one could as well imagine the formation of peroxides by adsorption of the dioxygen molecule on the bare surface followed by a dissociation. The dissociated oxygen could then in turn form a bond with existing surface oxygen leading to two peroxides at the surface. However, due to the high computational cost of DFT the latter case has not been studied in the present work.
Once the peroxide formed, regardless through which pathway, it has to be further reduced and incorporated into the LSCF slab. The incorporation process might be realized through a surface or sub-surface oxygen vacancy. In order to probe whether oxygen dissociation in the presence of a sub-surface is spontaneous, a structural optimization of a configuration with a peroxide and a sub-surface oxygen vacancy at NN position was carried out. After the relaxation, the peroxide stayed trapped in its initial position suggesting that incorporation due to a sub-surface oxygen vacancy has to be energetically activated and is thus not a spontaneous process.

Conclusion

DFT calculations have been performed on (100) AO-terminated slab models for LSCF for two different Cobalt contents (y=10.25 and y=0.25) and for different numbers of Strontium atoms (7 Sr and 8 Sr). The oxygen vacancy formation were studied for surface, sub-surface and sub-sub-surfaces. Formation energies were found to be positive with values between 1.3 to 2.2 eV. Thus, the formation of oxygen vacancies in LSCF present an endothermic process at 0K. The slab models have been used to investigate the interaction of the dioxygen molecule with the bare surface and surface oxygen vacancies. The surface oxygen vacancies present particular reactive sites for the oxygen gas adsorption with adsorption energies of the order of -1.3 to -2.3 eV. During the adsorption into the oxygen surface, the molecule is reduced and the bond length increased to a value typical for a peroxide state.

Acknowledgments

The work has been supported by the PTC simulation program at CEA (SOLSTIS project), Genvia and the CELCER-EHT project of the National Research Agency (ANR). This work was granted access to the HPC resources of TGCC under the project number A0130913833 made by GENCI.

References

1. K. Chen, S.P. Jiang, Surface Segregation in Solid Oxide Cell Oxygen Electrodes: Phenomena, Mitigation Strategies and Electrochemical Properties. *Electrochem. Energ. Rev.* **3**, 730–765 (2020).
2. J. Laurencin, M. Hubert, D. Ferreira Sanchez, S. Pylypko, M. Morales, A. Morata, B. Morel, D. Montinaro, F. Lefebvre-Joud, E. Siebert, Degradation mechanism of La0.6Sr0.4Co0.2Fe0.8O3-δ/Gd0.1 e0.9O2-δ composite electrode operated under solid oxide electrolysis and fuel cell conditions, *Electrochimica acta*, 241, 459-476, (2017)
3. H. Ding, A. V. Virkar, M. Liu and F. Liu, Suppression of Sr surface segregation in $La_{1-x}Sr_xCo_{1-y}Fe_yO_{3-\delta}$: a first principles study, *Chem. Phys*., 15, 489, (2013)
4. R. Gao, A. Fernandez, T. Chakraborty, A. Luo, D. Pesquera, S. Das, G. Velarde, V. Thoréton, J. Kilner, T. Ishihara, S. Nemšák, E. J. Crumlin, E. Ertekin, L. W. Martin, Correlating Surface Crystal Orientation and Gas Kinetics in Perovskite Oxide Electrodes. *Adv. Mater.*, 33, 2100977, (2021)
5. X. Gonze, F. Jollet, F. Abreu Araujo, D. Adams, B. Amadon, T. Applencourt, C. Audouze, J.-M. Beuken, J. Bieder, A. Bokhanchuk, E. Bousquet, F. Bruneval, D. Caliste, M. Cote, F. Dahm, F. Da Pieve, M. Delaveau, M. Di Gennaro, B. Dorado, C. Espejo, G. Geneste, L. Genovese, A. Gerossier, M. Giantomassi, Y. Gillet, D. Hamann, L. He, G. Jomard, J. Laflamme Janssen, S. Le Roux, A. Levitt, A. Lherbier, F. Liu, I. Lukacevic, A. Martin, C. Martins, M. Oliveira, S. Poncé, Y. Pouillon, T. Rangel, G.-M. Rignanese, A. Romero, B. Rousseau, O. Rubel, A. Shukri, M. Stankovski, M. Torrent, M. VanSetten, B. Van Troeye, M. Verstraete, D. Waroquiers,J. Wiktor, B. Xu, A. Zhou, and J. Zwanziger, Computer Physics Communications 205, 106 (2016)
6. F. Jollet, M. Torrent, N. Holzwarth, *Comput. Phys. Commun*. **185**, 1246-1254 (2014)
7. J. P. Perdew, K. Burke, and M. Ernzerhof, Generalized gradient approximation made simple, *Phys. Rev. Lett.* 77, 3865 (1996)
8. F. Jollet, G. Jomard, B. Amadon, J. P. Crocombette, and D. Torumba, Hybrid functional for correlated electrons in the projector augmented-wave formalism: Study of multiple minima for actinide oxides, *Phys. Rev. B* 80, 235109 (2009)
9. E. Effori, J. Laurencin, E. Da Rosa Silva, M. Hubert, T. David, M. Petitjean, G. Geneste, L. Dessemond and E. Siebert, *J. Electrochem. Soc.*, 168 (4), 044520 (2021)
10. L.-W. Tai, M.M. Nasrallah, H.U. Anderson, D.M. Sparlin, S.R. Sehlin, Structure and electrical properties of $La_{1-x}Sr_xCo_{1-y}Fe_yO_3$. Part 2. The system La1−xSrxCo0.2Fe0.8O3, *Solid State Ionics*, 76, 273-283, (1995)
11. C. Hartmann, J. Laurencin, and G. Geneste, Hole polarons in $LaFeO_3$ and $La_{1-x}Sr_xFeO_{3-\delta}$: Stability, trapping, mobility, effect of Sr concentration, and oxygen vacancies, Phys. Rev. B 107, 024104 (2023)